

## Molecular aggregates in cryogenic solutions

M. W. Schauer, J. Lee, and E. R. Bernstein

Citation: *The Journal of Chemical Physics* **76**, 2773 (1982); doi: 10.1063/1.443379

View online: <http://dx.doi.org/10.1063/1.443379>

View Table of Contents: <http://aip.scitation.org/toc/jcp/76/6>

Published by the *American Institute of Physics*

---

---

**COMPLETELY  
REDESIGNED!**



**PHYSICS  
TODAY**

*Physics Today* Buyer's Guide  
Search with a purpose.

# Molecular aggregates in cryogenic solutions<sup>a)</sup>

M. W. Schauer, J. Lee, and E. R. Bernstein

Colorado State University, Department of Chemistry, Fort Collins, Colorado 80523  
(Received 17 July 1981; accepted 25 November 1981)

Spectra of pyrazine, benzene, and osmium tetroxide have been obtained in cryogenic solutions. Data indicate that mixtures ( $\sim 10$  ppm solute in solvent) deposited at low temperatures ( $\sim 100$  K) yield clusters of solute molecules. The size of these clusters are estimated from light scattering data to be of the order of  $10^3$  Å. In particular, molecular aggregates appear in pyrazine/ $C_3H_8$ , benzene/ $NF_3$ ,  $CF_4$ ,  $OsO_4/C_3H_8$ ,  $NF_3$  but not in benzene/ $C_3H_8$ . The major factor governing the appearance of aggregates at low temperature is solubility. Upon warming these solutions to  $\sim 150$  K only solution spectra are observed; subsequent equilibrium cooling, of course, yields only precipitate.

## I. INTRODUCTION

Aggregates have been observed in a variety of solution systems. Often their formation is due to a Coulombic attraction between solute molecules. Such aggregates have been generated and partially characterized in dye solutions<sup>1</sup> and aqueous solutions of DNA bases and nucleic acids.<sup>2</sup> Hydrogen bonding can be a major factor in aggregate formation under these circumstances. Molecular aggregate formation associated with processes of nucleation and precipitation are viewed in a different light, however. In these processes, Coulombic forces do not typically predominate; the association of solute molecules is due to molecular crystal type dispersion or van der Waals forces. Study of these weak intermolecular interactions in solution can help elucidate the nature of solutions and the mechanisms for the phenomena of precipitation and nucleation. In the course of studying cryogenic liquid solutions of simple organic and inorganic molecules, it has been possible to generate aggregates and investigate them spectroscopically.

Theoretical approaches to aggregates have centered on nucleation theory.<sup>3</sup> Small cluster formation, usually at high temperature and in dilute gases rather than dense condensed phases,<sup>4</sup> has been treated by a kinetic theory of condensation and Mayer theory.<sup>5</sup> Some work has been done involving calculation of surface potentials in a Lennard-Jones fluid, using Percus-Yevich and hypernetted chain equations and comparing these theoretical results to Monte Carlo computer simulations.<sup>6</sup> These considerations are probably not directly applicable to the situation found for aggregation at low temperature in solution.

While somewhat different than the situation discussed in this paper, spectroscopic and mass spectral studies have appeared on molecular clusters in the gas phase.<sup>7</sup> For the case in which solute aggregates are studied in the molecular jet system, such as  $(H_2O)_x$ ,  $(C_6H_6)_x$ , etc., these latter results are not unrelated to those presented here. Supersonic molecular jet spectra of various types of clusters have evidenced both red [ $(C_6H_6)_2$  and  $He_xC_2N_4H_2$ ] and blue ( $He_xI_2$ ) shifts from the unperturbed isolated solute molecular spectra. Such shifts are central to the identification of aggregates as will be shown below.

<sup>a)</sup>Supported in part by grants from NSF and ONR.

In this work, some general observations serve to distinguish solutions of aggregates from solutions of monomers. Rapid deposition into a precooled sample cell is required to generate an aggregate solution. Such a solution yields an absorption spectrum which is always red shifted from the absorption spectrum of a solution of monomers. Spectra of monomer solutions may be either red or blue shifted from that of the low pressure ( $\sim 1$  Torr) gas, however. The red shift of the aggregate system always parallels (but is not always identical to) that observed for a pure crystal at comparable temperatures. If typical aggregate solutions are warmed to more than 120 K, spectra corresponding to aggregates begin to decrease slowly in intensity and, concomitantly, features associated with monomer spectra begin to appear. Cooling a solution of monomers shows that this process is, of course, not reversible; solute simply precipitates, as usual, without the reappearance of spectra associated with aggregate solutions. The aggregation process is trapped in a rapidly cooled and deposited nonequilibrium low temperature liquid. After several hours at low temperature (1–12 h, depending on the particular system), aggregate spectra begin to decrease in intensity and precipitate can be seen in the solution. The appearance of red shifted, temperature and time dependent spectra allows identification of an aggregate solution.

In this report, experimental procedures and results concerning the study of aggregates are presented. Absorption spectra of solutions of the following solutes and solvents have been studied: pyrazine/ $C_3H_8$ ; benzene/ $NF_3$ ,  $C_3H_8$ ,  $N_2$ ,  $CO$ ,  $CF_4$ ; and osmium tetroxide/ $NF_3$ ,  $CH_4$ ,  $C_3H_8$ . In order to obtain some qualitative estimation of aggregate size, light scattering experiments were also performed on solutions of pyrazine/ $C_3H_8$ , benzene/ $CF_4$ , benzene/ $NF_3$ , and benzene/ $C_3H_8$ . The nature of these nonequilibrium molecular clusters in solution will be addressed.

## II. EXPERIMENTAL

Purification and sample handling procedures for these experiments are similar to those reported previously.<sup>8</sup> Purification of solutes was accomplished by trap to trap vacuum distillation through molecular sieve. Solvents are in general similarly treated,<sup>8</sup> being distilled through a 130 K molecular sieve trap directly into an

outgassed 7 l stainless steel holding can. For light scattering experiments, the solvent distillation is done twice. Solvent and solute are mixed in the vapor phase in the holding can which then is allowed to equilibrate for at least 24 h before deposition to ensure thorough mixing of the two constituents. Deviation from this mixing procedure, however, did not yield different results for aggregate spectra.

The absorption apparatus is the same as that described previously. Solutions were held at set temperature between 65 and 220 K by a closed cycle mechanical refrigerator, and irradiated with a 500 W Xenon lamp filtered with various appropriate Hoya glass filters placed in water. A cooled RCA C31000M photomultiplier tube with photon counting electronics is used to detect the absorption.

Light scattering experiments use an argon ion laser with an intracavity etalon for single mode 5145 Å output. Powers at the sample are typically about 50 mW. Brillouin and Rayleigh (correlation) scattering are observed simultaneously in order to determine the best portion of the scattered light to detect for Rayleigh studies. This apparatus is described elsewhere.<sup>9</sup> The best correlation spectra are observed in the case for which Brillouin peaks are maximized in intensity, with respect to the central Rayleigh peak observed through the interferometer. Correlation light scattering is detected through two pin holes (100 μm) separated by about 0.5 m, with the first pinhole about 0.25 m from the collection lens. Scattered light is analyzed by a Malvern real time auto correlator and an HP 9845S computer for curve fitting and graphic output.

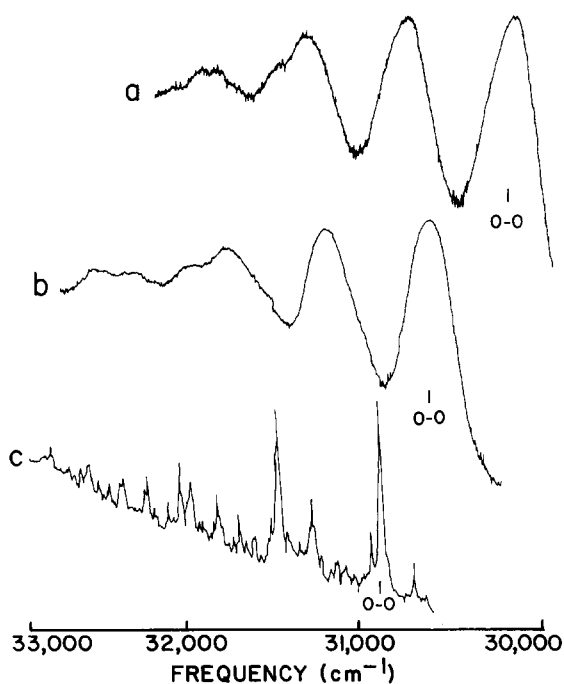


FIG. 1. Absorption spectra of pyrazine in propane: (a) aggregate spectrum at 100 K; (b) monomer spectrum at 150 K and (c) vapor spectrum at 300 K.

TABLE I. Assignments, energies, and gas to liquid red shift for solutions of pyrazine in propane. Errors in absolute energies are estimated to be  $\pm 15 \text{ cm}^{-1}$ .

| Assignment        | Energy ( $\text{cm}^{-1}$ ) | Red shift from gas phase ( $\text{cm}^{-1}$ ) |
|-------------------|-----------------------------|---|
| Aggregate (100 K) |                             |   |
| $^1B_{3u}$ origin | 30 057                      | 819   |
| $6a_0^1$          | 30 646                      | 813   |
| $6a_0^2$          | 31 227                      | 815   |
| $8a_0^1$          | 31 406                      | 843   |
| $6a_0^3$          | 31 786                      | 839   |
| $8a_0^1 6a_0^1$   | 31 989                      | 843   |
| Solution (150 K)  |                             |   |
| origin            | 30 562                      | 314   |
| $6a_0^1$          | 31 142                      | 316   |
| $6a_0^2$          | 31 723                      | 319   |
| $8a_0^1$          | 31 933                      | 316   |
| $6a_0^3$          | 32 299                      | 326   |
| $8a_0^1 6a_0^1$   | 32 503                      | 329   |
| Gas (300 K)       |                             |   |
| origin            | 30 876                      |   |
| $6a_0^1$          | 31 459                      |   |
| $6a_0^2$          | 32 042                      |   |
| $8a_0^1$          | 32 249                      |   |
| $6a_0^3$          | 32 625                      |   |
| $8a_0^1 6a_0^1$   | 32 832                      |   |

### III. RESULTS

Absorption spectra of pyrazine in propane at  $\sim 100 \text{ K}$  evidence the characteristics associated with aggregate solutions described earlier. These data show the  $^1B_{3u}$  origin of pyrazine shifted  $505 \text{ cm}^{-1}$  to the red of the monomer (150 K) origin and  $819 \text{ cm}^{-1}$  to the red of the gas phase origin<sup>10</sup> (see Fig. 1). Aside from this overall shift the three spectra, gas, monomer solution, and aggregate solution spectra are superimposable. Assignments of vibronic features are indicated in Fig. 1 and Table I.

Warming the low temperature solution causes the aggregate spectrum to decrease in intensity. As the aggregate spectrum disappears, the monomer spectrum begins to appear and increases in intensity until reaching its equilibrium value. Upon subsequent cooling of the solution back to 100 K, aggregate spectra do not reappear: monomer spectra and some precipitate are observed. No spectra can be observed associated with any amount of precipitate floating in solution.

Spectra were also obtained as a function of concentration. At 100 K, only monomer spectra are seen for 3.5, 5, and 7 ppm, and below 2 ppm no spectra were observed at all. At 8 ppm, clear pyrazine/propane

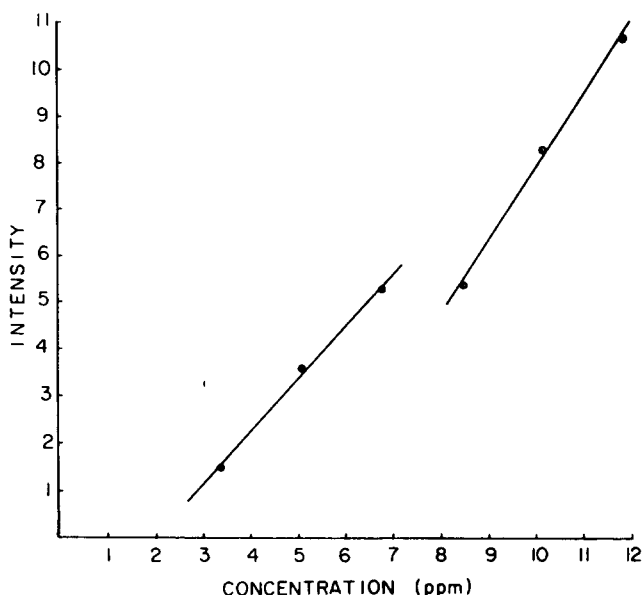


FIG. 2. Plot of intensity of the absorption spectra measured as the height of the origin peak vs concentration of pyrazine in propane deposited at 100 K. The first three points correspond to monomer spectra and the last three points correspond to aggregate spectra.

solutions show aggregate spectra, and concentrations of 10, 12, and 14 ppm yield aggregate spectra of increased intensity. A graph of this concentration-intensity dependence at fixed temperature is given in Fig. 2.

Light scattering experiments were carried out on pyrazine/propane and benzene/NF<sub>3</sub>, CF<sub>4</sub>, C<sub>3</sub>H<sub>8</sub> solutions in order to estimate mean aggregate size.<sup>9</sup> A relaxation curve of the decay of the time correlation function for the system can be fit to a single exponential decay function (Fig. 3); from this process, a relaxation time may be calculated. Using the relations

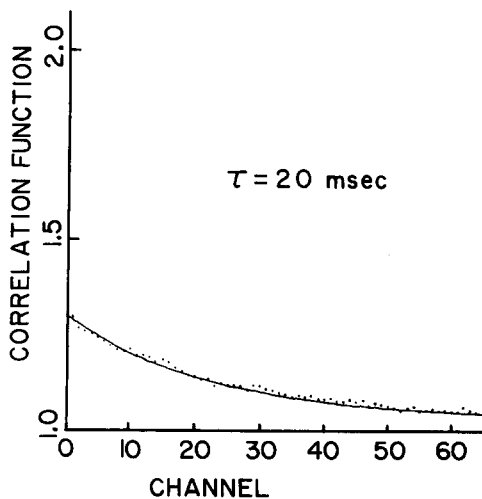


FIG. 3. Plot of the normalized correlation function for a solution of pyrazine aggregates in propane at 3.5 ppm and 100 K. The solid line is a least squares fit to a single exponential function yielding a correlation time of  $\tau = 20$  ms.

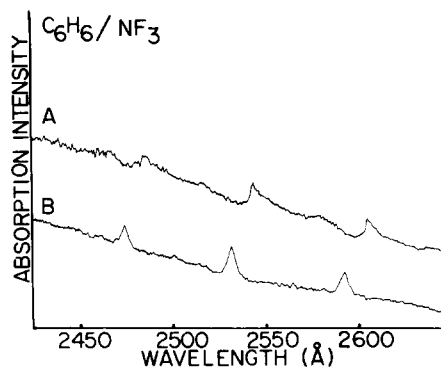


FIG. 4. Spectra of benzene in NF<sub>3</sub>: (A) aggregate solution (8 ppm) spectra taken at 90 K; (B) monomer solution (8 ppm) taken at 140 K.

$$1/\tau = Dq^2, \quad D = \frac{kT}{6\pi\eta_r a}, \quad q^2 = 4\left(\frac{2\pi\eta_r}{\lambda}\right)^2 \left(\sin \frac{\theta}{2}\right)^2,$$

in which  $\tau$  = relaxation time,  $D$  = diffusion constant,  $q$  = scattering vector,  $k$  = Boltzmann's constant,  $T$  = temperature,  $\eta_v$  = viscosity,  $a$  = particle diameter,  $\eta_r$  = refractive index for 5145 Å,  $\lambda$  = wavelength of light, and  $\theta$  = scatter angle ( $\theta = 90^\circ$ ); a particle size can be calculated assuming a spherical particle shape. The observed relaxation for the pyrazine/C<sub>3</sub>H<sub>8</sub> aggregate solution, at  $100 \pm 10$  K and independent of concentration from 3.5 to 15 ppm, is found to be  $20 \pm 2$  ms. This corresponds to a particle size of roughly  $10^3$  Å. Similar results are obtained for benzene/NF<sub>3</sub> and CF<sub>4</sub> but no aggregates are found in C<sub>6</sub>H<sub>6</sub>/C<sub>3</sub>H<sub>8</sub> solution at any temperature.

Solution and aggregate spectra for C<sub>6</sub>H<sub>6</sub>/NF<sub>3</sub> are presented in Fig. 4, which shows the temperature dependence of the spectra of an 8 ppm sample. The aggregate spectrum was obtained in a 90 K solution and the monomer spectrum was obtained in a 140 K solution. Table II summarizes the assignments for both aggregates and monomers.

Figure 5 depicts three spectra of the first two one photon allowed bands of OsO<sub>4</sub>: gas phase at 300 K, monomer solution at 150 K in C<sub>3</sub>H<sub>8</sub>, and aggregate solution of NF<sub>3</sub> at 90 K. Figure 6 shows monomer and aggregate spectra of OsO<sub>4</sub> in C<sub>3</sub>H<sub>8</sub> at 150 and 120 K, re-

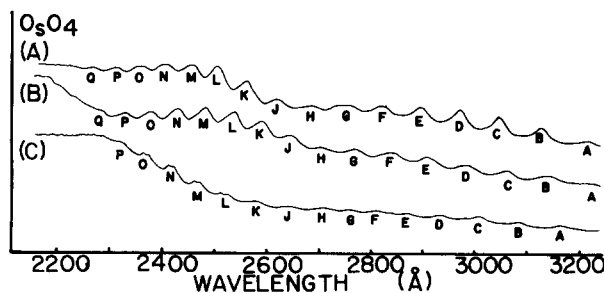


FIG. 5. Absorption spectra of OsO<sub>4</sub>: (A) OsO<sub>4</sub>/C<sub>3</sub>H<sub>8</sub> monomer spectrum at 8 ppm and 150 K; (B) OsO<sub>4</sub>/NF<sub>3</sub> aggregate spectrum at 8 ppm and 90 K; and (C) OsO<sub>4</sub> gas phase spectrum at 4°C [notation of Ref. 12(b) is employed here and in the text].

TABLE II. Absorption data for  $C_6H_6$  in  $NF_3$  at 90 K (aggregate) and 140 K (monomer solution). Gas phase data are also given for comparison. All values are in  $cm^{-1}$ .

| Gas phase<br>300 K | Solution (140 K) |                     | Aggregate (90 K) |                     | Assignment    |
|--------------------|------------------|---------------------|------------------|---------------------|---------------|
|                    | Frequency        | Gas to liquid shift | Frequency        | Gas to liquid shift |               |
| 38 612             | 38 531           | -81                 | 38 318           | -294                | $6_0^1$       |
| 39 534             | 39 451           | -83                 | 39 250           | -284                | $6_0^1 1_0^1$ |
| 40 456             | 40 381           | -75                 | 40 181           | -275                | $6_0^1 1_0^2$ |

spectively. In comparison to the gas phase spectrum, two distinct regions may be classified in these condensed phase spectra. In monomeric solutions, the first six bands show a red shift with respect to the gas phase spectrum, while the last 12 bands evidence a blue shift from the corresponding gas phase values. For aggregate solutions ( $C_3H_8$  and  $NF_3$ ), all bands are red shifted, however, by varying amounts from the gas phase spectrum but in such a manner as to preserve this decomposition. These data are summarized in Table III.  $OsO_4$  is itself not soluble enough in  $NF_3$  to produce an observable monomer solution spectrum at 140 K.

#### IV. DISCUSSION

The most extensive study of solute aggregate formation is for pyrazine; both absorption and light scattering measurements have been made for this system at many temperatures and concentrations. In the discussion given below, most phenomena will be presented for pyrazine; observations dealing with  $C_6H_6$  and  $OsO_4$  solutions will be presented only as they pertain to these individual systems.

##### A. Pyrazine

The red shift of the pyrazine aggregate spectrum is close to that of the pyrazine crystal spectrum.<sup>11</sup> This indicates that aggregation provides an environment similar to that found in the crystal.

The deposition procedure has been observed to be im-

portant for the production of aggregates. If mixtures are cooled slowly under equilibrium conditions, precipitation ensues without observable amounts (in absorption or light scattering experiments) of aggregate production. With rapid, nonequilibrium deposition, supersaturated solutions are produced which trap aggregates in solution and prevent precipitation. As the temperature is raised above 120 K for  $C_4N_2H_4/C_3H_8$ , aggregates are broken up by increased solubility of monomers and the overall increase in  $kT$ . Of course, both energy and entropy considerations control the solvation process.

Linewidths for the aggregate spectra are roughly as one might expect; similar to a pure crystal at  $\sim 100$  K. The lack of emission from aggregate species is also understandable in this light. The implication, as shown below, is that most aggregates are fairly large with  $n \geq 10^3$ . The fact that (hydrocarbon) solution and aggregate linewidths are similar may be indicative of similar short range repulsive interactions in both systems. The long range forces, due mostly to C-C and C-N potentials, are, of course, different in aggregate and solution, as is evident from the different gas to liquid and gas to aggregate red shifts for pyrazine.

Light scattering experiments demonstrate that there is a sharp decrease in the size of scatters with an increase in temperature. At roughly 140 K, nearly all the aggregates have dissolved and the number density of effective scatters has decreased to the point at which trace amounts of dust become the primary scatters. Single pyrazine molecules are too small to be observed in this experiment.

The two different techniques for observing the presence of aggregates in solution, absorption and light scattering, have distinct sensitivities for each of the solution species. For example, at low concentrations ( $< 5$  ppm), absorption spectra show no aggregate peaks but light scattering indicates the presence of  $10^3$  Å size particles. At about 5-7 ppm, monomer absorption is

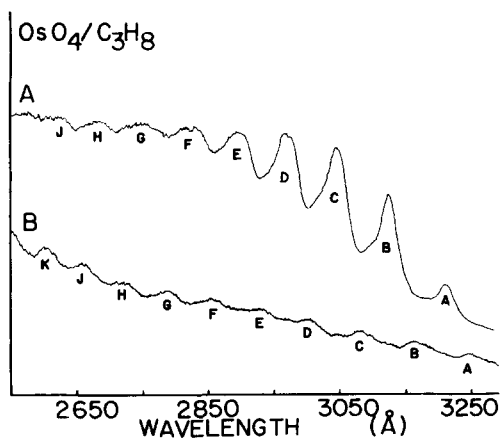


FIG. 6. Absorption spectra of  $OsO_4/C_3H_8$ : (A) monomer spectrum at 60 ppm and 150 K, and (B) aggregate spectrum at 60 ppm and 120 K.

TABLE III. Average gas to liquid shift for  $OsO_4$  in  $cm^{-1}$ .

| Bands <sup>a</sup> | Solvents            |                       |                     |
|--------------------|---------------------|-----------------------|---------------------|
|                    | $C_3H_8$<br>Monomer | $C_3H_8$<br>Aggregate | $NF_3$<br>Aggregate |
| A-F                | -144                |                       |                     |
| G-R                | 228                 | -286                  | -211                |

<sup>a</sup>Labels in Figs. 5 and 6 and Ref. 12(b).

obscured by aggregate features (Fig. 1). Near 15 ppm,  $C_4N_2H_4/C_3H_8$  microcrystals can be observed floating in solution at 100 K. Upon warming these solutions to 150 K and subsequently cooling them, neither technique can observe aggregates, even under conditions for which precipitate can be visually observed floating in solution. Monomers are still observed in absorption but light scattering data are unattainable.

Within experimental error, the size of aggregate particles in solution does not depend significantly on concentration; high concentrations of pyrazine simply produced stronger light scattering but always with roughly the same relaxation time. Higher concentration solutions are observed, however, to yield precipitation at higher temperatures.

Size determination of aggregates is most likely an order of magnitude estimate. There are two major sources of error. The primary source of error is probably the assumption of spherical shape, which leads to a diameter of  $10^3$  Å. A sphere of this diameter would include of the order of  $10^6$  pyrazine molecules. If the particles are disk or cylinder shaped, the number of molecules per particle could be several orders of magnitude less. Moreover, a different shape would yield a different relationship between measured relaxation time and effective particle size. The most probable shape of these aggregates is, of course, not known; however, hints taken from rapid crystallization processes could favor cylindrical rods with large length to diameter ratios. A further complication for the determination of particle size is that there may exist in solution a broad continuum or distribution of sizes. If this were the case, one might expect that size distribution for a given solution would depend fairly strongly on initial concentration. This was certainly not observed in any of the light scattering experiments in the concentration range 3–15 ppm. It may well be, however, that average relaxation times are not sensitive enough to changes in the most probable size distribution to evidence this polydispersivity. Thus, the measured times may be dominated by the largest particles in the distribution.

## B. Benzene

The previous report from our laboratory on cryogenic liquid solutions dealt with the first excited singlet state of benzene<sup>9</sup>; aggregates were not identified for  $C_6H_6$  in CO,  $N_2$ ,  $CF_4$ ,  $CH_4$ ,  $C_2H_6$ , and  $C_3H_8$ . Nonetheless,  $C_6H_6/NF_3$  solutions clearly show that at low temperature aggregation of  $C_6H_6$  does indeed occur with a size close to that determined for pyrazine. The monomer spectrum (Fig. 2, bottom) of  $C_6H_6/NF_3$  shows two solvent effects which distinguish this system from other  $C_6H_6$  solutions: a small ( $\sim 80$   $cm^{-1}$ ) gas to liquid shift and a small band width (FWHM  $\sim 100$   $cm^{-1}$ ). Other solvents produce roughly 200  $cm^{-1}$  linewidths and  $\sim 275$   $cm^{-1}$  gas to liquid shifts. In addition, this spectrum behaves much like that described for the pyrazine monomer: it is stable, reversible, and independent of deposition procedure. Again, linewidths and gas to aggregate shifts strongly suggest a close similarity between the aggregate and crystalline state and an aggregate size of  $n \geq 10^6$ .

Appearance of aggregate spectra for  $C_6H_6/NF_3$  (Fig. 2 and Table II) raises questions concerning spectra of  $C_6H_6$  in other solutions.<sup>8</sup> In the case of the solvents  $C_2H_6$  and  $C_3H_8$ , all spectra observed can be attributed to monomers for the following three reasons: (1) both solvents have high boiling points and thus are good solvents (the calculated solubility at 150 K is roughly  $4 \times 10^{-2}$ ); (2) spectra are completely temperature independent; and (3) spectra of  $C_6H_6/C_2H_6$  or  $C_3H_8$  are time independent at any temperature between 85 and 200 K. Due to the high solubility of  $C_6H_6$  in these two solvents, it is quite unlikely that the aggregation phenomenon can be observed. In fact, light scattering experiments reveal no detectable particle size at low temperature, thus eliminating the possibility that the monomer and aggregate spectra overlap.

CO,  $N_2$ ,  $CF_4$ , and  $CH_4$  on the other hand, have low boiling points and are relatively poor solvents for benzene. Moreover, the short liquid range makes it quite difficult to study temperature dependent spectra and gas to liquid and gas to crystal (aggregate) shifts are quite similar for these systems ( $\sim -250$   $cm^{-1}$ ). Unfortunately, light scattering studies for these systems are difficult to perform because the low solubility usually yields some particulate matter even at low concentrations.

## C. OsO<sub>4</sub>

Aggregation of  $OsO_4$  is also found in  $C_3H_8$  and  $NF_3$  solvents at 90 K. Both sets of features (A through F and G through R in Figs. 5 and 6 and in Table III) now evidence a red shift. Such results show that the  $OsO_4$  aggregates, and indeed other aggregates in general, are crystal-like and not as affected by the solvent environment as monomers are.

The observation of both red (lower energy bands A through F) and blue (higher energy bands G through R) shifts for solution spectra with respect to gas phase spectra of  $OsO_4$  (see Table III and Fig. 5) raises the question of the appropriate assignment of these transitions. These shift data clearly divide the bands into two electronic transitions. The two one photon allowed lowest observed  $OsO_4$  transitions have been frequently discussed with respect to their orbital origin. It seems generally agreed that the first transition takes an electron from the highest filled  $1t_1$  orbital to the lowest unfilled  $2e$  orbital;  $T_1$  and  $T_2$  states are thereby created.<sup>12</sup> The second transition may involve either  $1t_1$  to unfilled  $4t_2$  or  $3t_2$  (second highest filled orbital) to  $2e$ . The  $2e$  and  $4t_2$  orbitals are essentially nonbonding metal  $d$  orbitals split by the  $O_4^{8-}$  tetrahedral crystal field. Presently, the  $(3t_2 - 2e) T_2$  assignment appears to be favored.<sup>13</sup> While it is clear that these two transitions involve different orbital sets, it is not apparent from the gas to liquid shift data which set is to be preferred for the higher energy one.

## V. CONCLUSION

The major point made in this presentation is that, for low temperature deposition and poor solvents, a supersaturated nonequilibrium situation obtains in which aggregates of solute are formed as a precursor to com-

plete precipitation. Aggregates are recognized by light scattering-particle size determination and by characteristic large crystal-like red shifts from both gas phase and solution spectra. Further studies are underway to elucidate the nature of the nucleation and growth process and to determine the actual shape(s) of such systems.

- <sup>1</sup>B. H. Robinson, A. S. Löffler, and G. Schwarz, *J. Chem. Soc. Faraday Trans. 1* **71**, 815 (1975).
- <sup>2</sup>S. I. Chan, M. P. Schweizer, P. O. P. Ts'o, and G. K. Helmkamp, *J. Am. Chem. Soc.* **86**, 4182 (1964).
- <sup>3</sup>(a) E. R. Buckle, *Faraday Discuss. Chem. Soc.* **61**, 7 (1976); (b) M. R. Hoare and J. McInnes, *ibid.* **61**, 12 (1976).
- <sup>4</sup>E. Donaghue and J. H. Gibbs, *J. Chem. Phys.* **74**, 2975 (1981).
- <sup>5</sup>A. M. Lockett III, *J. Chem. Phys.* **72**, 4822 (1980).
- <sup>6</sup>Y. Singh and F. F. Abraham, *J. Chem. Phys.* **67**, 537 (1977).
- <sup>7</sup>(a) D. H. Levy, L. Wharton, and R. E. Smalley, *Chemical and Biochemical Applications of Lasers* (Academic, New York, 1977), Vol. II, pp. 1-41; (b) A. W. Castleman, Jr., P. M. Holland, and R. G. Keesee, *J. Chem. Phys.* **68**, 1760 (1978); (c) R. R. Gamache and P. E. Cade, *ibid.* **74**, 5197 (1981); (d) M. P. Casassa, D. S. Bomse, and K. C. Janda, *ibid.* **74**, 5044 (1981).
- <sup>8</sup>E. R. Bernstein and J. Lee, *J. Chem. Phys.* **74**, 3159 (1981).
- <sup>9</sup>B. J. Berne and R. Pecora, *Dynamic Light Scattering* (Wiley, New York, 1976).
- <sup>10</sup>Y. Udagawa, M. Ito, and I. Suzuka, *Chem. Phys.* **46**, 237 (1980).
- <sup>11</sup>E. F. Zalewski, D. S. McClure, and D. L. Narva, *J. Chem. Phys.* **61**, 2964 (1974).
- <sup>12</sup>(a) K. Swift and E. R. Bernstein, *J. Chem. Phys.* **74**, 5981 (1981); (b) E. J. Wells, A. D. Jordan, D. S. Alderdice, and I. G. Ross, *Aust. J. Chem.* **20**, 2315 (1967).
- <sup>13</sup>(a) E. Diemann and A. Müller, *Chem. Phys. Lett.* **19**, 538 (1973); (b) J. L. Roebber, R. N. Wiener, and A. Russell, *J. Chem. Phys.* **60**, 3166 (1974); (c) P. Quested, D. J. Robbins, P. Day and R. G. Denning, *Chem. Phys. Lett.* **22**, 158 (1973).